

# Excess Pore Water Pressure Ratio Comparison from Empirical and Numerical Methods to Determine Liquefaction Potential in Palu, Central Sulawesi, Indonesia



Mukhlis Habib Al Rahman<sup>1</sup>, Teuku Faisal Fathani<sup>1,\*</sup> and Wahyu Wilopo<sup>2</sup>

<sup>1</sup>Department of Civil and Environmental Engineering, Universitas Gadjah Mada, Yogyakarta, Indonesia

<sup>2</sup>Department of Geological Engineering, Universitas Gadjah Mada, Yogyakarta, Indonesia

## Abstract:

**Background:** Palu is a city in Central Sulawesi Province with a very high level of seismic activity. The seismicity in Central Sulawesi is associated with the active movement of the Palu Koro fault. One of the most severe events occurred on September 28, 2018, which triggered liquefaction and a tsunami. This is also related to the lithology of Palu, which consists of alluvial deposits predominantly made up of sand.

**Objective:** This study compares excess pore water pressure values analyzed empirically and numerically to identify liquefaction potential. It aims to provide additional perspectives for engineers in designing buildings around the study area that are resistant to liquefaction.

**Methods:** Excess pore water pressure was analyzed using empirical and numerical methods to determine liquefaction potential. The empirical method used the equation by Yegian and Vitteli (1981), while the numerical method involved finite element analysis using the Plaxis 2D application and nonlinear analysis using DEEPSOIL v7.

**Results:** The results from the three methods of analyzing excess pore water pressure to determine liquefaction potential at the four borehole points showed differences. For the empirical method, using the equation by Yegian and Vitelli (1981), the results indicated that the layers with a pore pressure ratio ( $r_v > 0.8$ ) were deeper than the finite element and non-linear methods.

**Conclusion:** The differences in methods result in varying outcomes in analyzing excess pore water pressure to identify liquefaction potential. The empirical method uses the peak value of Peak Ground Acceleration (PGA) to evaluate the entire soil profile, leading to a more generalized assessment. In contrast, the non-linear and finite element methods consider each layer's behavior under the applied seismic load, providing more detailed and similar results.

**Keywords:** Excess pore water pressure, PM4Sand, DEEPSOIL v7, Liquefaction potential, Safety factor, Site response analysis.

© 2025 The Author(s). Published by Bentham Open.

This is an open access article distributed under the terms of the Creative Commons Attribution 4.0 International Public License (CC-BY 4.0), a copy of which is available at: <https://creativecommons.org/licenses/by/4.0/legalcode>. This license permits unrestricted use, distribution, and reproduction in any medium, provided the original author and source are credited.

\*Address correspondence to this author at the Department of Civil and Environmental Engineering, Universitas Gadjah Mada, Yogyakarta, Indonesia; E-mail: [tfathani@ugm.ac.id](mailto:tfathani@ugm.ac.id)

Cite as: Al Rahman M, Fathani T, Wilopo W. Excess Pore Water Pressure Ratio Comparison from Empirical and Numerical Methods to Determine Liquefaction Potential in Palu, Central Sulawesi, Indonesia. Open Civ Eng J, 2025; 19: e18741495372949. <http://dx.doi.org/10.2174/0118741495372949250114055629>



Received: November 22, 2024

Revised: December 02, 2024

Accepted: December 10, 2024

Published: January 17, 2025



Send Orders for Reprints to  
[reprints@benthamscience.net](mailto:reprints@benthamscience.net)

## 1. INTRODUCTION

Palu is located in an area of high seismicity, especially due to its location along the Palu Koro fault line. This fault

is one of the most active faults in Indonesia and is prone to earthquakes. The Palu Koro fault extends from Central Sulawesi to the Moluccas Sea, and the area it crosses,

including the city of Palu, is prone to earthquakes due to active fault movement.

The earthquake that struck the city of Palu on September 28, 2018, triggered a tsunami and liquefaction disaster. A total of 2,200 people were reported dead, with 1,000 missing and 4,500 injured [1]. This disaster is the largest in the history of Palu City.

Liquefaction is a phenomenon where sandy soil experiences shocks that cause a sudden increase in pore water pressure, causing the loss of bonds between soil particles. As a result of the loss of these bonds, the soil loses its strength and stiffness, so it cannot support the load of the structure built on it.

The level of liquefaction susceptibility is important in planning a building in areas with sandy soil and high seismic activity. This factor influences the design of foundations suitable for supporting the building during liquefaction.

According to Indonesia's Liquefaction Susceptibility Zone, Palu City has a very high liquefaction potential [2]. This is due to the city's soil lithology, which consists of alluvial and coastal deposits with materials such as sand, silt, and coral [3]. In addition to its sand-dominated lithology, Palu City experiences very high seismic activity, further contributing to its high liquefaction potential.

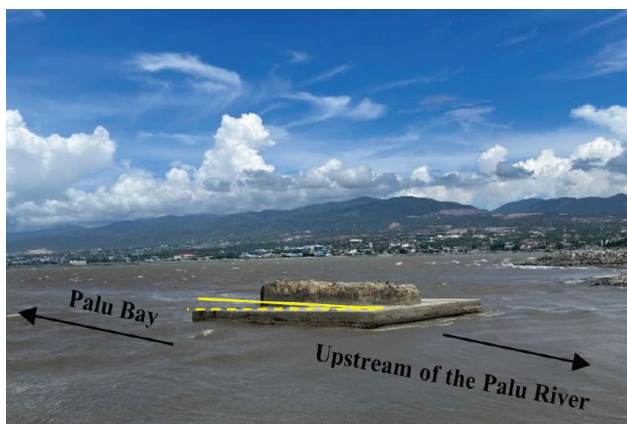


**Fig. (1).** Pile cap on the pier of the old bridge that has collapsed.

The calculation of liquefaction analysis is supported by the discovery of liquefaction phenomena in the study area. In the research conducted by Sassa and Takagawa in 2018 [4], characteristics indicating that the study area experienced liquefaction were found, including sand boils around the bridge structures. During the study, other phenomena were also observed, such as changes in the inclination of the pile cap on the old bridge pier, which collapsed during the 2018 event, as demonstrated in Fig. (1). Additionally, it was found that the foundation of the retaining wall near the study location experienced deformation, as illustrated in Fig. (2).

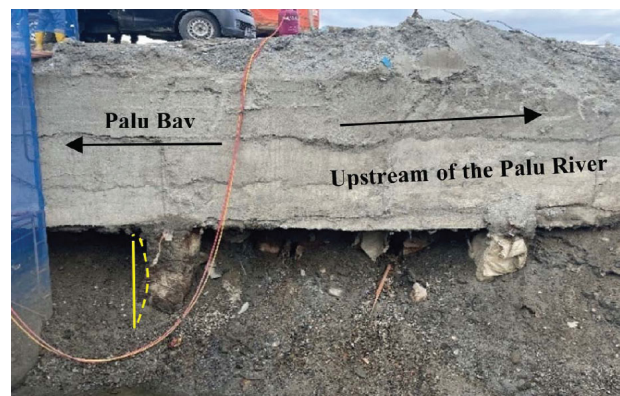


**Fig. (2).** Foundation structure of the retaining wall on the palu river.

Research on liquefaction potential analysis has been extensively conducted. Generally, liquefaction potential analysis uses the Standard Penetration Test (SPT) parameter, with the output being a comparison between the Cyclic Resistance Ratio (CRR) and the Cyclic Stress Ratio (CSR) [5]. CRR refers to the cyclic resistance ratio of the soil to withstand shear stress during an earthquake, while CSR represents the shear stress caused by the earthquake that could lead to soil liquefaction.

The study site is located on the eastern bank of the downstream Palu River. Research related to liquefaction risk based on excess pore water pressure ratio values at the study site has never been conducted, making it an interesting subject for investigation. Similar studies were performed on the Balaroa area, with a potential liquefaction level reaching 9 m, the Petobo area, with a 6–10 m depth, and the Jono Oge area, with a potential liquefaction depth reaching 17 m [6].

This study analyzes liquefaction potential by comparing the excess pore water pressure values obtained from empirical calculations and numerical calculations using the Plaxis 2D and DEEPSOIL v7 applications. The Peak Ground Acceleration (PGA) parameter refers to the 2017 Earthquake Hazard and Source Map, with a 7% probability of exceedance in 75 years [7].

## 2. MATERIALS AND METHODS

### 2.1. The Research Area

The research area is located downstream of the river in the eastern part of Palu City. This study is based on four soil investigation borehole points, BH 1, BH 2, BH 3, and BH 4, as shown in Fig. (3). The Palu 4 Bridge is being constructed in the research area, specifically on the eastern side abutment and embankment.

### 2.2. Geological and Geotechnical Condition

The research location consists of alluvial and coastal deposits. Its position downstream of the Palu River results in sediment transport quite far from the weathering source, leading to sand grains with rounded shapes. The

rounded grain shape reduces the interlocking between particles. Additionally, these deposits formed during the

Quaternary period, meaning the sediments' cementation process has not yet occurred [8].

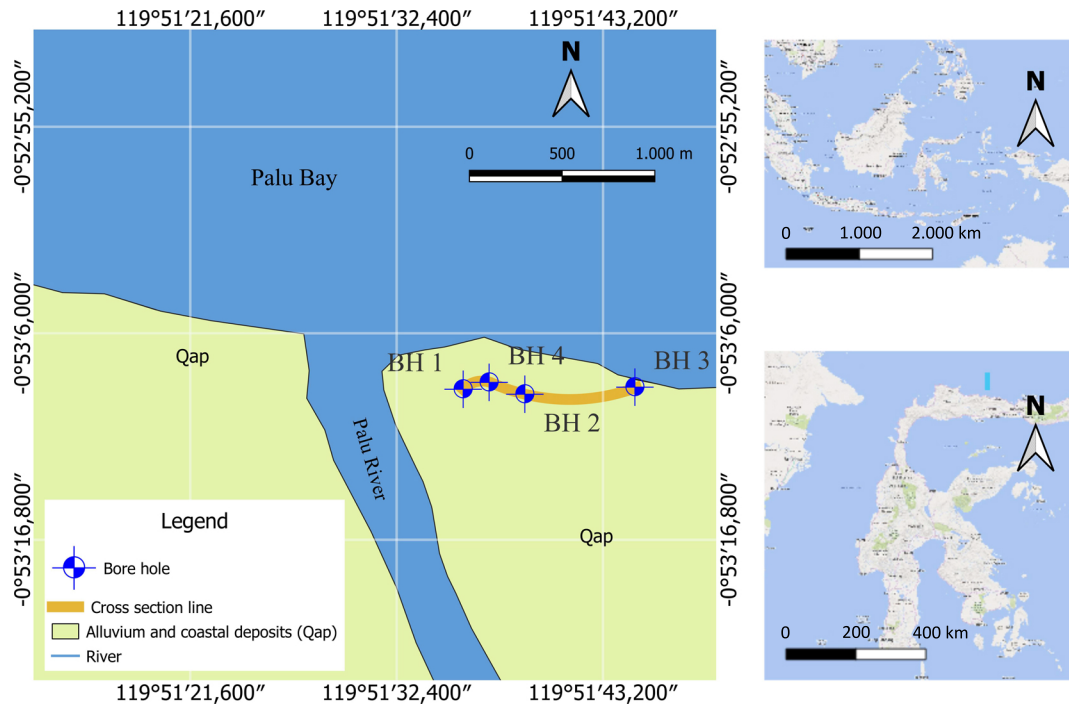


Fig (3). Borehole location in the research area [3].

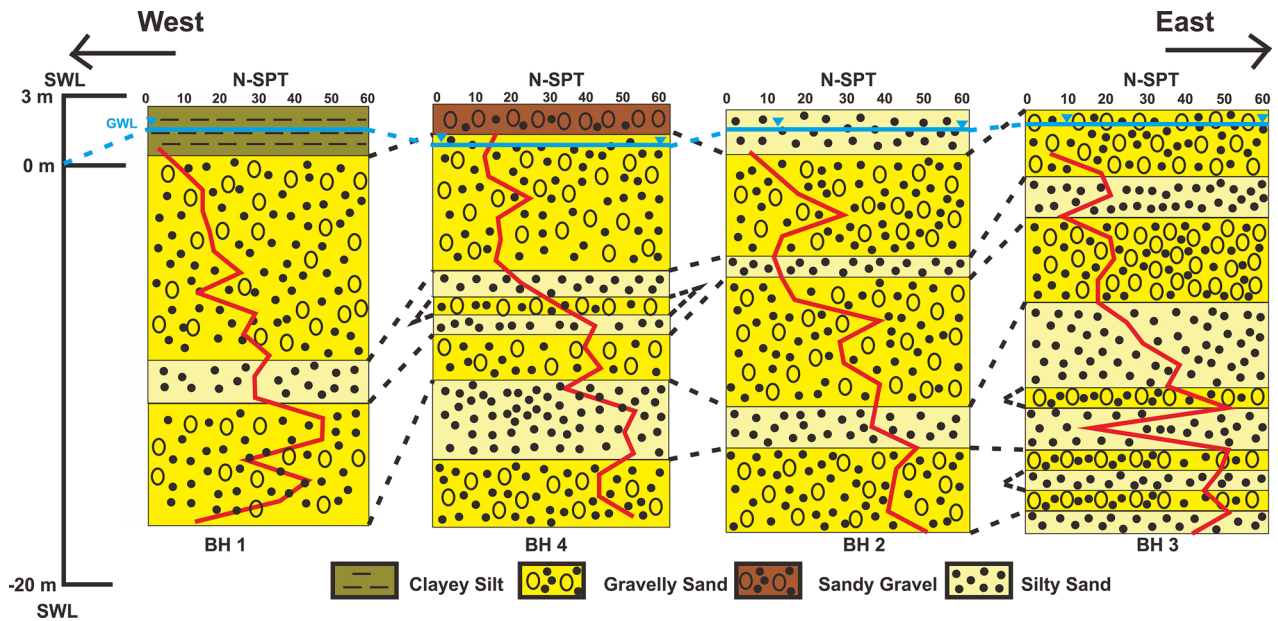


Fig. (4). The cross-sectional profile of soil layers extending from west to east.

Palu City is located along the Palu Koro Fault, a strike-slip fault that moves at a rate of 42 mm per year [9]. This movement is associated with the high seismic activity in the area. The research location is at the mouth of the Palu River, which is directly connected to Palu Bay, resulting in a shallow groundwater table. With sandy soil, high seismic activity, and a shallow groundwater level, there are early indications that the research location is prone to liquefaction.

Based on the sieve analysis results, the lithology of the four borehole points indicates that the lithology consists of clayey silt and sandy gravel up to a depth of 20 meters. The NSPT values at the four borehole points vary, ranging from 6 to 50, as shown in Fig. (4). The four borehole points have different groundwater levels: BH 1 has a groundwater depth of 1.1 m with a drilling elevation of 2.72 m above sea level, BH 2 has a depth of 1.05 m with a drilling elevation of 2.52 m above sea level, BH 3 has a depth of 0.6 m with a drilling elevation of 2.54 m above sea level, and BH 4 has a depth of 1.74 m with a drilling elevation of 3.08 m above sea level.

### 2.3. Data Acquisition

The data consists of soil investigation data from Standard Penetration Test (SPT) values from four boreholes: BH 1, BH 2, BH 3, and BH 4. This study also utilizes laboratory test data.

The ground motion data used are earthquake recordings from the Pacific Earthquake Engineering Research Center (PEER) via the website <https://ngawest2.berkeley.edu/>, with input parameters derived from deaggregation using the Indonesian Earthquake Hazard Deaggregation Map for Seismic-Resistant Infrastructure Planning and Evaluation [10]. Once determined, the ground motion matches the target design spectra created based on the Indonesian National Standard 2833:2016 [11].

### 2.4. Data Analysis

The field measurement data from the Standard Penetration Test (SPT) is corrected using several correction factors, such as overburden pressure correction, correction for the energy ratio produced by the hammer blow, borehole diameter correction, SPT rod length correction, fine grain content correction, and correction for the liner of the SPT sampler [12].

After applying the corrections to the SPT values, the next step is calculating the Cyclic Resistance Ratio (CRR) with a correction factor for effective overburden pressure correction ( $K_\sigma$ ). The earthquake magnitude used is 7.5 Mw, referring to the Palu earthquake that occurred on September 28, 2018. The CRR value is calculated using Eq. (1) mentioned below [13].

$$CRR_{M,\sigma'v} = CRR_{M=7.5,\sigma'=1} \cdot MSF \cdot K_\sigma, \quad (1)$$

where  $CRR_{M,\sigma'v}$  represents the CRR value that has been corrected with the magnitude scaling factor ( $MSF$ ) and the effective overburden pressure correction ( $K_\sigma$ ).

The factor of safety against liquefaction requires the analysis of the Cyclic Stress Ratio (CSR) using Eq. (2). The CSR is calculated using the Peak Ground Acceleration (PGA) value of 0.794g from the Indonesian Seismic Code, with a 7% probability of exceedance over 75 years. The total vertical stress influences the CSR value ( $\sigma_v$ ), effective vertical stress ( $\sigma'_v$ ), maximum ground acceleration due to the earthquake, gravitational acceleration ( $g$ ), and the stress reduction factor ( $r_d$ ). The equation is as follows:

$$CSR_{M,\sigma'v} = 0.65 \frac{\sigma_v a_{max}}{\sigma'_v g} r_d. \quad (2)$$

The Safety Factor (SF) value is the ratio between the CRR and CSR values, as shown in Eq. (3) below.:

$$SF = \frac{CRR_{M,\sigma'v}}{CSR_{M,\sigma'v}}. \quad (3)$$

The Boulanger and Idriss (2014) method is commonly used for identifying liquefaction potential. This method can be applied using data that are typically available, such as N-SPT values, as well as laboratory test data commonly performed, such as specific gravity, plasticity index for silt and clay, and sieve analysis. Therefore, the Simplified Procedures method is the most suitable empirical method for this research.

The obtained safety factor results are then processed using the equation given by Yegian and Vittelli in 1981 [14] to determine the excess pore water pressure ratio ( $r_u$ ), as shown in Eq. (4) below, where  $\alpha$  and  $\beta$  values are 0.7 and 0.19, respectively.

$$r_u = \frac{2}{\pi} \arcsin \left( \frac{1}{SF} \right)^{\frac{1}{2\alpha\beta}}. \quad (4)$$

The Yegian and Vittelli (1981) method presents the results of the simplified procedure calculations from Boulanger and Idriss (2014), which are expressed as the excess pore water pressure ratio ( $r_u$ ) to facilitate comparison with the nonlinear and finite element methods. These comparison results will be part of the analysis in this study. Although this method was introduced many years ago, it is still widely used by several recent authors [15-17].

The target spectra are determined using the PGA value, the spectral value at the ground surface for a 1-second period ( $S_{DS}$ ), and the spectral value at the ground surface for a short period of 0.2 seconds ( $S_{D1}$ ). The value of  $S_{DS}$  is obtained from <https://lini.binamarga.pu.go.id/> based on reference [9]. Several parameters are needed to establish the target spectra to define the curve boundaries. The first parameter required is the initial transition period from the phase of maximum acceleration ( $T_0$ ), followed by the transition period where spectral acceleration starts to decrease as the period increases ( $T_s$ ). After the period  $T_s$ , the spectral acceleration ( $S_i$ ) is determined. These parameters can be calculated using Eqs. (5-7), given as follows:

$$T_0 = 0,2 T_s, \quad (5)$$

$$T_s = \frac{S_{D1}}{S_{DS}}, \tag{6}$$

$$S_a = \frac{S_{D1}}{T}. \tag{7}$$

After determining the target spectrum, matching is performed so that the ground motion can be adjusted to field conditions. The matching results are shown in Fig. (5). The results of the ground motion matching that has been performed can be seen in Fig. (6).

### 2.5. Nonlinear Site Response Analysis

Numerical analysis is conducted as a comparison to

the empirical method [14, 15]. Numerical analysis can be performed using 1-D Site Specific Response Analysis (SSRA) with the DEEPSOIL v7 application to estimate the excess pore water pressure. This analysis uses the Generalized Quadratic/Hyperbolic (GQ/H+PWP) approach.

The main parameters for numerical analysis using DEEPSOIL v7 with the Dorby and Matasovic Model Parameters for sand layers are normalized excess pore pressure ( $U_N$ ), equivalent number of cycles ( $>N_{eq}$ ), current reversal shear strain ( $>\gamma_c$ ), threshold shear strain value ( $>\gamma_{tvp}$ ), curve fitting parameters (P, s, and F), dimensionality factor (f), and degradation parameter (v).

### Matched Ground Motion

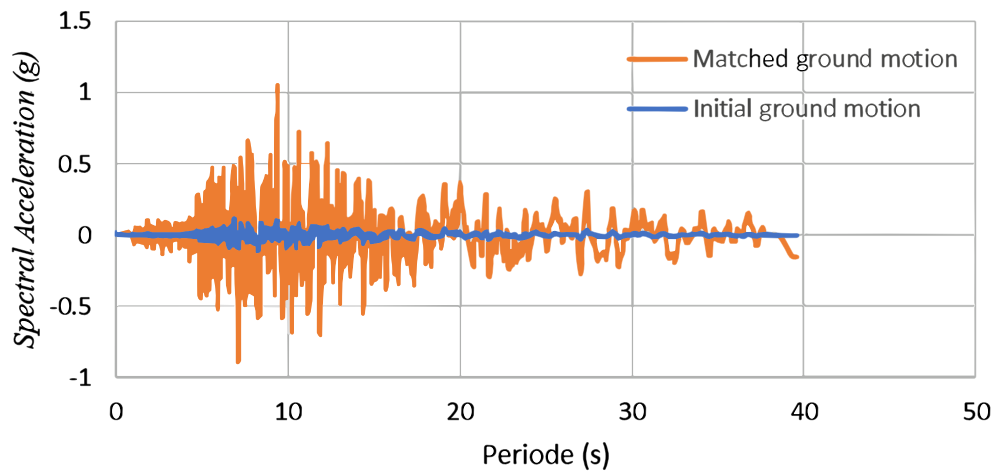


Fig. (5). Comparison of target response spectrum and matched response spectrum results.

### Matched Response Spectrum

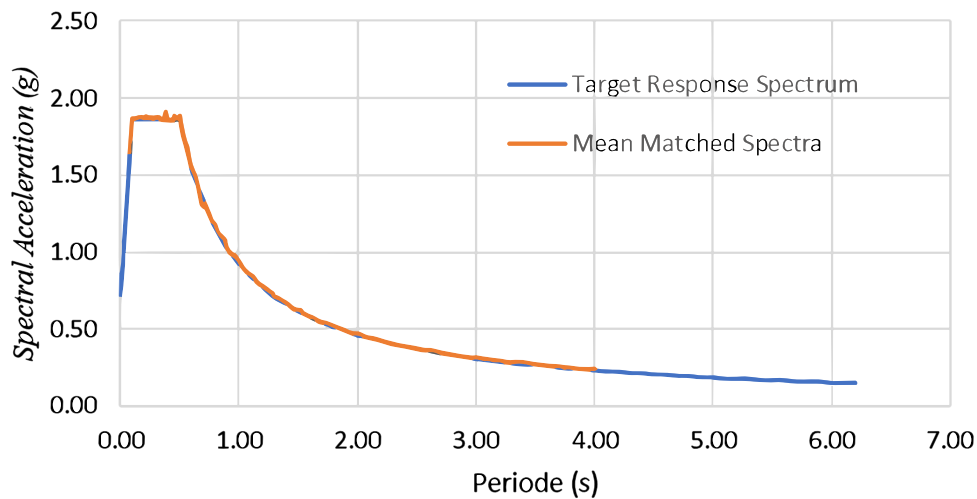


Fig. (6). Comparison of initial ground motion and matched ground motion results.

In its calculations, this model is influenced by the Fines Content (FC) and shear wave Velocity ( $V_s$ ) values [18], as shown in Eqs. (8) and (9) below:

$$s = (FC + 1)^{0.1252}, \quad (8)$$

$$F = 3810 V_s^{-1.55}. \quad (9)$$

The parameter  $v$  is calculated using Eq. (10) given below, where  $D_r$  represents the relative density in %.

$$v = 1 < 0.078 D_r - 2.53 < 3.8 \quad (10)$$

For clay layers, the Matasovic and Vucetic (1995) model parameters are used, with key parameters including normalized excess pore pressure ( $U_N$ ), equivalent number of cycles ( $N_{eq}$ ), current reversal shear strain ( $\gamma_c$ ), threshold shear strain value ( $\gamma_{vp}$ ), curve fitting parameters ( $r$  and  $s$ ), and curve fitting coefficients ( $A$ ,  $B$ ,  $C$ , and  $D$ ). The values for each parameter are based on Matasovic and Vucetic (1995) for marine clay material (OCR 1.0).

The  $r_u$  analysis using the nonlinear method is performed to account for the nonlinear behavior of the soil during an earthquake. The PGA value, which is one of the triggers of liquefaction, will be adjusted according to the soil response. This method is used to determine the amplification of earthquake vibrations, which in turn increases pore water pressure, leading to liquefaction.

## 2.6. Finite Element Method

Excess pore water pressure can be calculated numerically using the Plaxis 2D application with the PM4Sand model. Plaxis 2D utilizes the finite element method to analyze and estimate the increase in pore water pressure. PM4Sand simulates the behavior of sand under dynamic conditions, which generates the values of pore water pressure increase, liquefaction conditions, and displacement values following the dynamic event [19].

The main parameters in the PM4Sand model are atmospheric pressure ( $pA$ ), contraction rate parameter ( $h_{po}$ ), shear modulus ( $G_o$ ), and relative density ( $D_R$ ) [20]. The atmospheric pressure value used is 101.3 kPa.

The relative density ( $D_R$ ) parameter is obtained using the equation from Idriss and Boulanger (2008) [21], with parameters including the corrected SPT value at 1 atm overburden ( $(N_1)_{60}$ ) and other values as shown in Eq. (11) below:

$$D_R = \sqrt{\frac{(N_1)_{60}}{46}} \quad (11)$$

Shear modulus coefficient ( $G_o$ ) controls the small strain shear (elastic), the expression covering a range of typical densities can be used to calculate the parameter directly  $G_o$  as proposed by Boulanger and Ziotopoulou (2015) [22] in Eq. (12) given below:

$$G_o = 167 \sqrt{(N_1)_{60} + 2.5}. \quad (12)$$

The steps to obtain the contraction rate parameter require using the Cyclic Direct Simple Shear (CDSS) test.

This is conducted to calibrate the CRR value under cyclic conditions. Liquefaction is considered to occur when the peak shear strain reaches 3% after undergoing cycles in the CDSS test.

**Table 1. Parameters of PM4S and for sand.**

Parameter	Value	Unit
$\alpha$	0.096	-
$\beta$	0.00079	-
$e$	Laboratory data	-
$D_R$	Eqs.5	-
$G_o$	Eqs.6	-
$h_{po}$	CDSS testing	-
$pA$	101.3	kPa
$e_{max}$	0.8	-
$e_{min}$	0.5	-
$n^b$	0.5	-
$n^d$	0.1	-
$\phi_{cv}$	33	°
Q	10	-
R	1.5	-

The input parameters for the sand layer analysis using the PM4Sand model include unsaturated unit weight ( $\gamma_{unsat}$ ), saturated unit weight ( $\gamma_{sat}$ ), void ratio ( $e_{int}$ ), Rayleigh damping with a value of 0.096 for Rayleigh  $\alpha$  and 0.00079 for Rayleigh  $\beta$ , initial relative density ( $D_R$ ), shear modulus coefficient ( $G_o$ ), contraction rate ( $h_{po}$ ), atmospheric pressure ( $pA$ ), maximum void ratio ( $e_{max}$ ), minimum void ratio ( $e_{min}$ ), bounding surface position according to  $\xi_R(n^b)$ , bounding surface position according to  $\xi_R(n^d)$ , critical state friction angle ( $\phi_{cv}$ ), critical state line parameters for Q and R, and the earth pressure coefficient  $K_o$ , with each value as shown in Table 1.

**Table 2. Parameters of HS small for clay.**

Parameter	Value	Unit
$\alpha$	0.096	-
$\beta$	0.00079	-
$E_{50}^{ref}$	9,000	kN/m <sup>2</sup>
$E_{oed}^{ref}$	9,000	kN/m <sup>2</sup>
$E_{ur}^{ref}$	27,000	kN/m <sup>2</sup>
$m$	1	-
$C_{ref}$	30	kN/m <sup>2</sup>
$\phi'$	26	°
$\psi$	0	°
$\gamma_{0.7}$	0.0007	-
$G_o^{ref}$	60,000	kN/m <sup>2</sup>
$v_{ur}'$	0.2	-
$P_{ref}$	100	kN/m <sup>2</sup>
$K_0^{nc}$	0.5616	-
$C_{inc}'$	0	kN/m <sup>2</sup> /m
$Y_{ref}$	0	m
$R_f$	0.9	-
OCR	2	-

The parameters used for the clay layer utilize the HS small model. This model includes several input parameters such as secant stiffness in standard drained triaxial test ( $E_{50}^{ref}$ ), tangent stiffness for primary oedometer loading ( $E_{oed}^{ref}$ ), power for the stress-level dependency of stiffness ( $m$ ), cohesion ( $c_{ref}'$ ), friction angle ( $\phi'$ ), unloading/reloading stiffness ( $E_{ur}^{ref}$ ), dilatancy angle ( $\psi$ ), shear strain at which  $G_s = 0.722 G_o (\nu_{0.7})$  shear modulus at very small strains ( $G_0^{ref}$ ), Poisson's ratio ( $\nu_{ur}'$ ), reference stress ( $P_{ref}$ ), cohesion increment ( $c_{inc}$ ), reference coordinate ( $y_{ref}$ ), failure ratio ( $R_f$ ), and Over Consolidation Ratio (OCR), as demonstrated in Table 2.

the help of Plaxis 2D is employed to provide a more detailed simulation of the pore water pressure ratio increase during an earthquake. The finite element method divides the entire soil layers into smaller elements, allowing for more precise and accurate analysis.

This study is conducted in stages, starting with an analysis using an empirical method that simplifies the calculation process. Next, a non-linear method is applied to analyze each soil layer individually, providing a more detailed soil response compared to the empirical method. Finally, the finite element method is used to divide the entire soil layers into smaller elements, yielding more detailed and accurate results.

### 3. RESULTS AND DISCUSSION

#### 3.1. Liquefaction Potential Analysis using the Empirical Method

Liquefaction potential analysis at four borehole points was conducted using the simplified procedure introduced by Boulanger and Idriss (2014) [13]. The earthquake parameter used in the study was a magnitude of 7.5 Mw, which occurred in Palu City on September 28, 2018, with a PGA value of 0.794g. Liquefaction is unlikely to occur at depths greater than 20 meters [23]. A study by Iwasaki in 1981 on the liquefaction potential index also limits liquefaction potential to a depth of 20 meters [24]. Based on previous research, empirical analysis was conducted up to a depth of 20 meters.

The results of soil data processing using the simplified procedure by Boulanger and Idriss (2014) [13] indicate that borehole BH 1 has liquefaction potential up to a depth of 17 m, borehole BH 2 up to a depth of 12 m, borehole BH 3 up to a depth of 15 m, and borehole BH 4 up to a depth of 13.5 m, as shown in Fig. (7).

Excess pore water pressure calculation using the Yegian and Vitelli (1981) equation employs parameters such as the liquefaction safety factor value. Thus, for layers with liquefaction potential, the limit with an  $r_u$  value  $> 0.8$  is at the same depth as the  $SF$  value  $< 1$ , as shown in Fig. (8).

#### 3.2. Liquefaction Potential Analysis Using Numerical Methods

In conducting liquefaction risk analysis using numerical methods, ground motion is required as the earthquake load to observe the soil's response to seismic loading. This study used ground motion from the Imperial Valley earthquake in 1979, with a magnitude of 6.5 Mw and a strike-slip fault mechanism. This ground motion is then matched to the target spectrum to approximate the ground motion conditions at the research location.

At point BH 1, data processing using DEEPSOIL v7 shows that layers with an  $r_u > 0.8$  are located at depths of 6.5 m and 8.5 m, as shown in Fig. (9). The results also indicate an increase in Pore Water Pressure (PWP) ratio at 37.4 seconds for the 6.5 m layer and 37.2 seconds for the 8.5 m depth layer, as shown in Fig. (10). The liquefied layer is a gravelly sand layer with an average N-SPT value of 14 and 17.

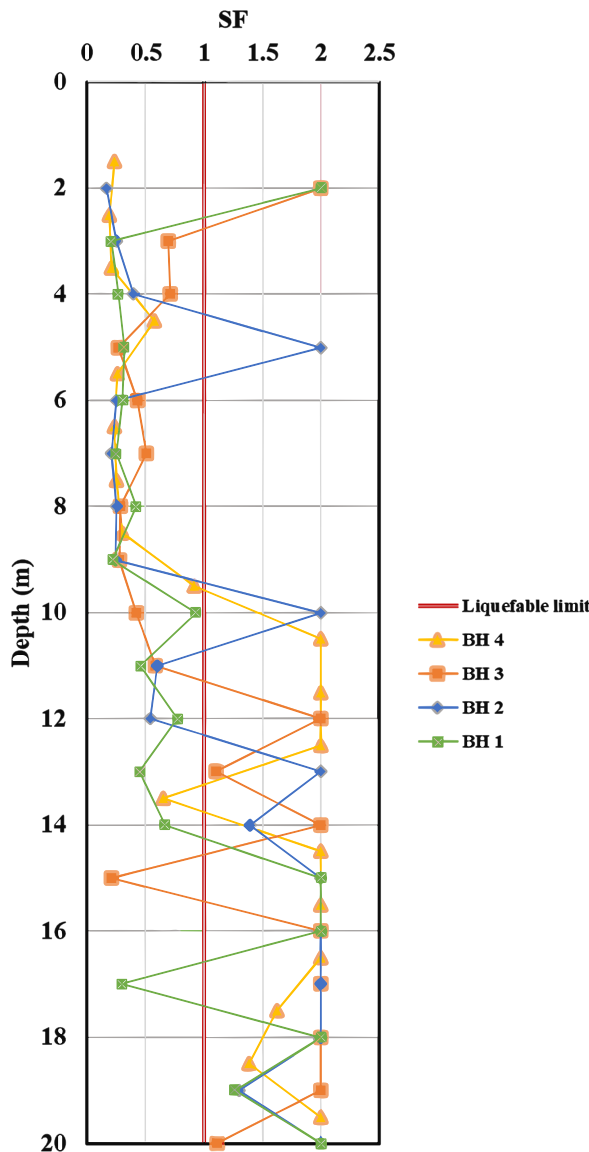


Fig. (7). Safety factor values for 4 borehole points.

The analysis of  $r_u$  using the finite element method with

At point BH 2, data processing with DEEPSOIL v7 shows an  $r_u > 0.8$  at a depth of 7 m, as shown in Fig. (11). The results also indicate that  $r_u > 0.8$  occurs at 21.6 seconds, as shown in Fig. (12). The liquefied layer is a silty sand to gravelly sand layer with an average N-SPT value of 14 and 17.

At point BH 3, data processing using DEEPSOIL v7 shows an  $r_u$  value  $> 0.8$  at depths of 4.5 m and 7.5 m, as shown in Fig. (13). The results also indicate an increase in  $r_u > 0.8$  at 20.8 seconds for the soil layer at a depth of 4.5 m and at 37.2 seconds for the soil layer at a depth of 7.5 m, as shown in Fig. (14). The liquefied layer is a silty sand to gravelly sand layer with average N-SPT values of 9 and 20.

At point BH 4, data processing with DEEPSOIL v7 shows an  $r_u > 0.8$  at a depth of 10 m, as shown in Fig. (15). The results also indicate that  $r_u > 0.8$  occurs at 35.7 seconds, as shown in Fig. (16). The liquefied layer is a gravelly sand layer with an average N-SPT value of 17.

The analysis results of the increase in pore water pressure ratio ( $r_u$ ) using the nonlinear method show that liquefaction occurs in the silty sand to gravelly sand layers with an N-SPT range of 9 to 20. In the time history analysis, liquefaction begins after 21 seconds.

A numerical analysis was conducted using another tool, Plaxis 2D, with the PM4Sand model to compare the numerical method. The results show that borehole GA 04 has an  $r_u > 0.8$  at 2-9 m depth, as shown in Fig. (17). The liquefied layer is a gravelly sand layer with an average N-SPT value of 9 and 17.

At borehole BH 2, liquefaction occurred down to a depth of 11 m. This is indicated by an  $r_u$  value greater than 0.8 at 3 m and 11 m depths, as demonstrated in Fig. (18). The liquefied layer consists of silty sand and gravelly sand layers with average N-SPT values of 6 and 17.

At borehole BH 3, liquefaction occurred down to a depth of 10 m. This is indicated by an  $r_u$  value greater than 0.8 at depths of 0-2 m, followed by depths of 4-5 m and 5-10 m, as shown in Fig. (19). The liquefied layer consists of silty sand and gravelly sand layers with average N-SPT values ranging from 6 to 20.

At borehole, BH 4, the Plaxis 2D calculations indicate a liquefied layer at a depth of 6.25 m. This is shown by an  $r_u$  value greater than 0.8 at a depth of 6.25 m, as illustrated in Fig. (20). The liquefied layer consists of gravelly sand with an average N-SPT value of 17.

The results obtained from the finite element method analysis indicate that the liquefied layer consists of silty sand to gravelly sand with N-SPT values ranging from 6 to 20. An interesting finding from the finite element method is that when a layer has a significant potential for liquefaction, with a thickness greater than the critical threshold, the  $r_u$  value exceeding 0.8 is not evenly distributed throughout the entire layer. Instead, the high  $r_u$  values are concentrated at the lower boundary of the layer.

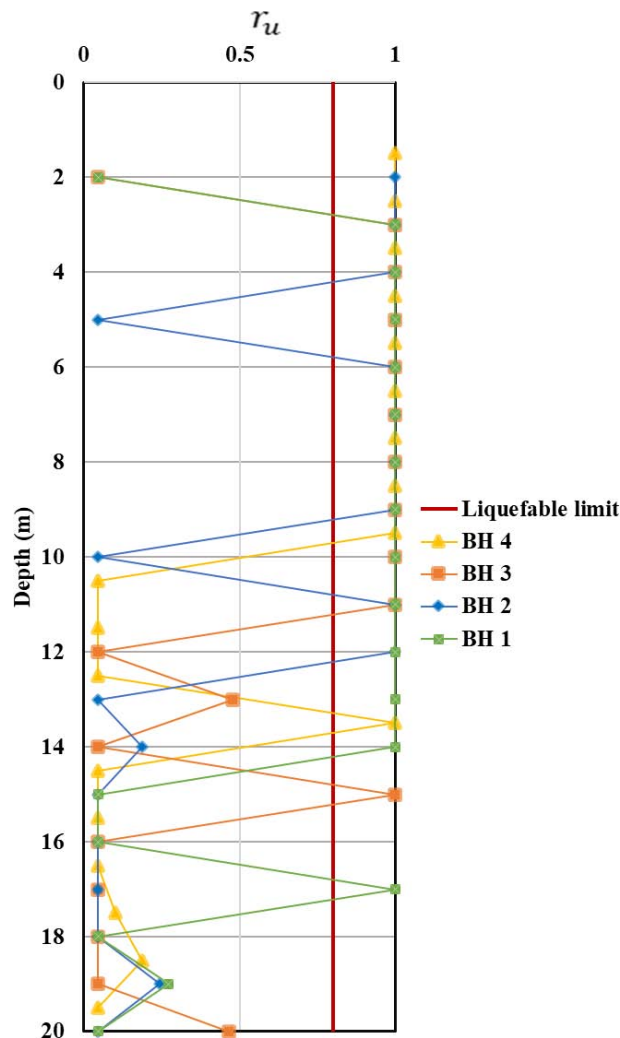


Fig. (8).  $r_u$  values for 4 borehole points using the Yegian and Vitelli (1981) method.

Table 3. Results of the analysis show the deepest layers with a pore pressure ratio ( $r_u > 0.8$ ).

Borehole	Yegian and Vitelli (1981)	DEEPSOIL v7	Plaxis 2D
BH 1	17 m	8.5 m	9 m
BH 2	12 m	11 m	11 m
BH 3	15 m	10 m	10 m
BH 4	13.5 m	13.95 m	6.25 m

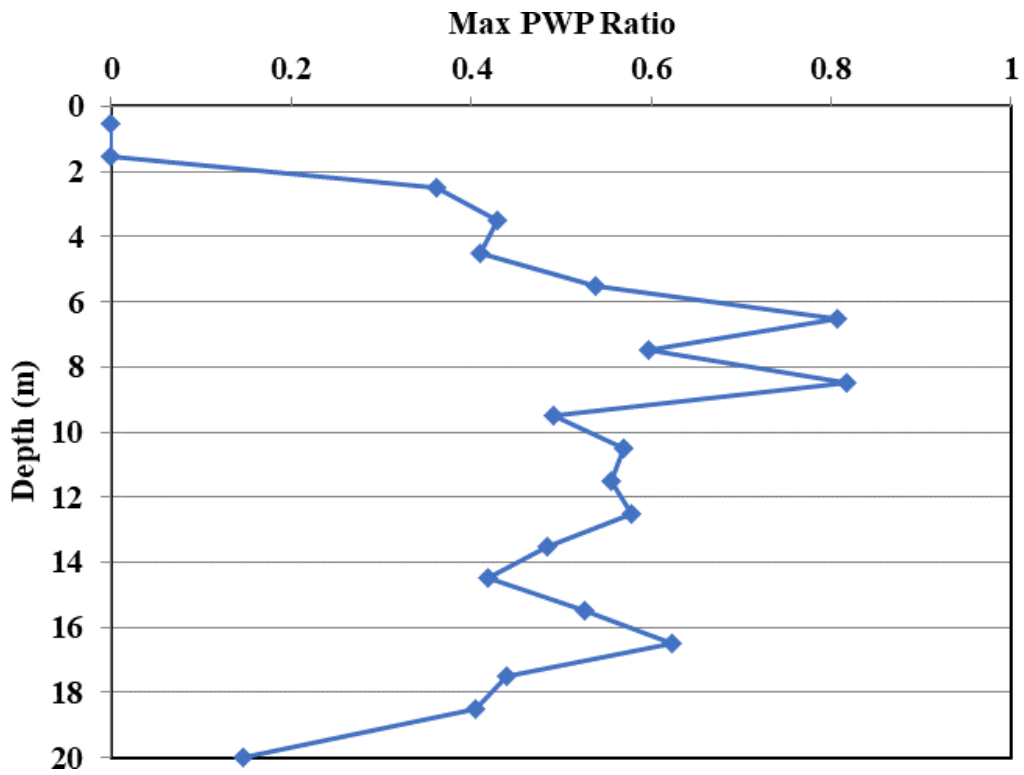


Fig. (9).  $r_u$  value at borehole BH 1.

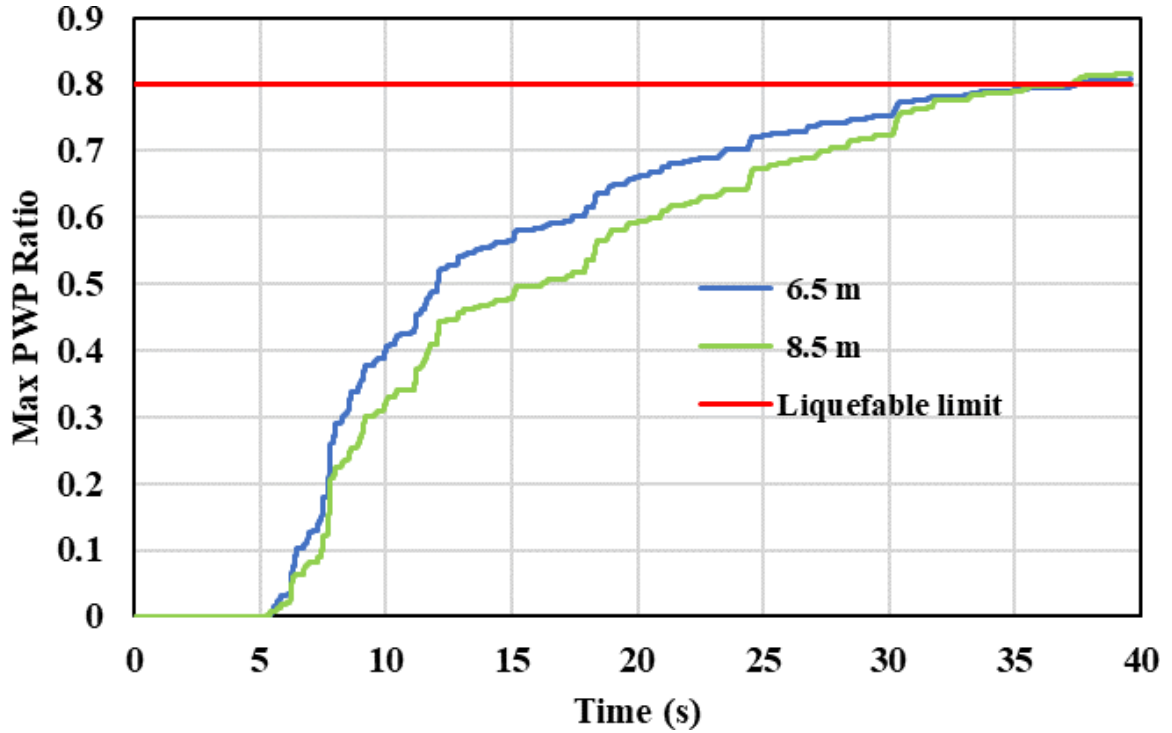


Fig. (10). Time history of  $r_u$  at borehole BH 1.

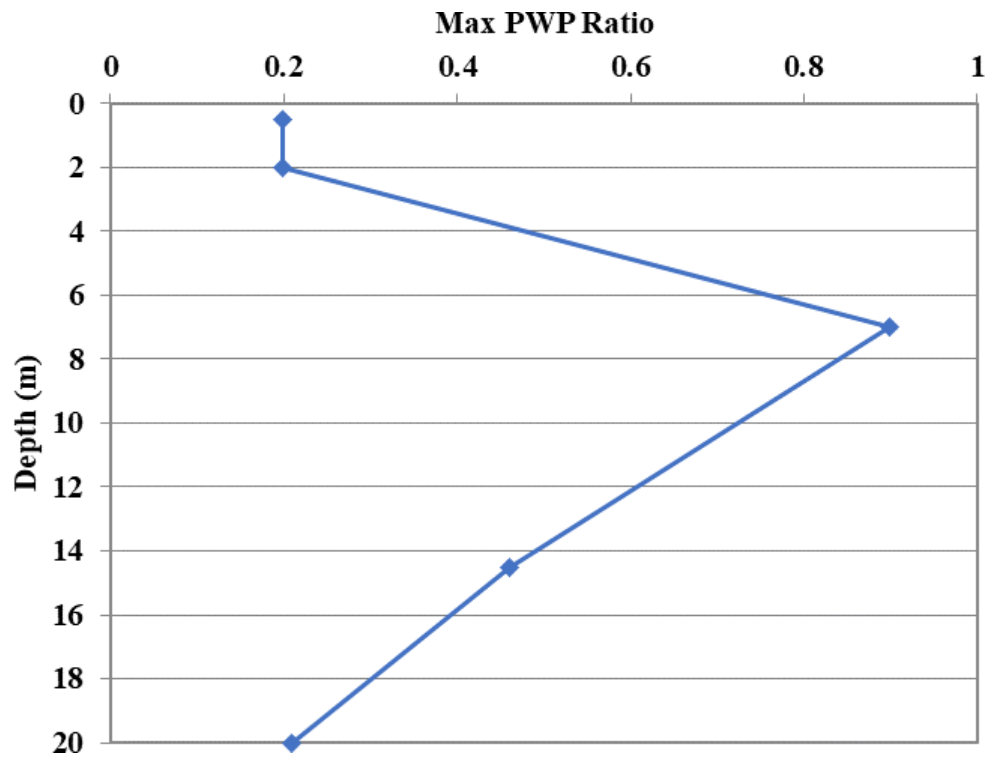


Fig. (11).  $r_v$  value at borehole BH 2.

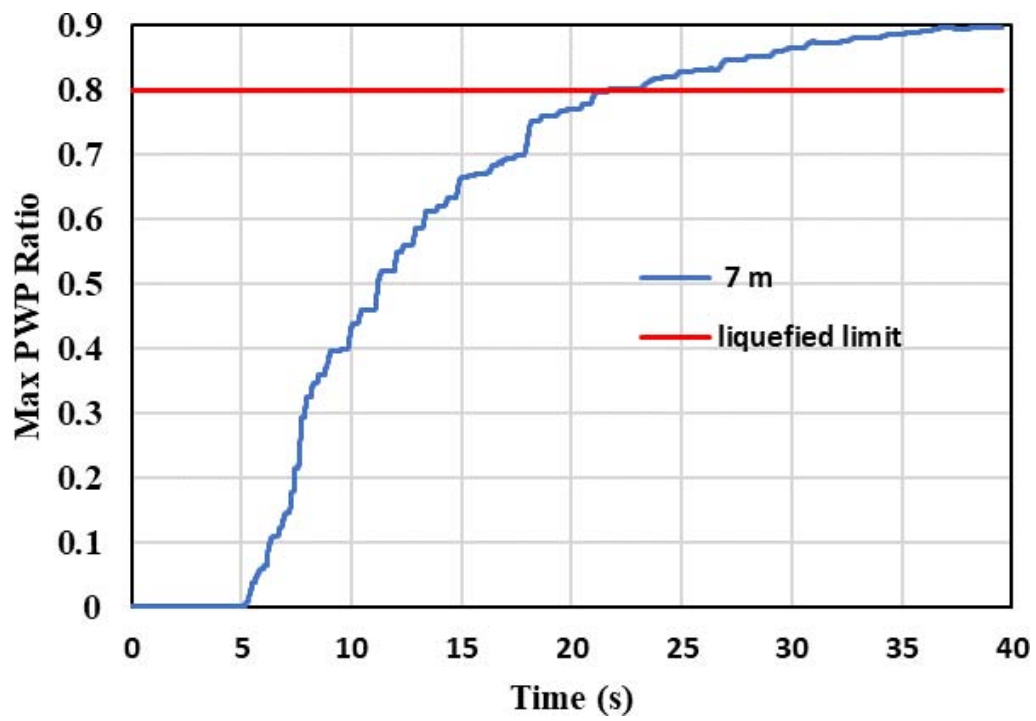


Fig. (12). Time history of  $r_v$  at borehole BH 2.

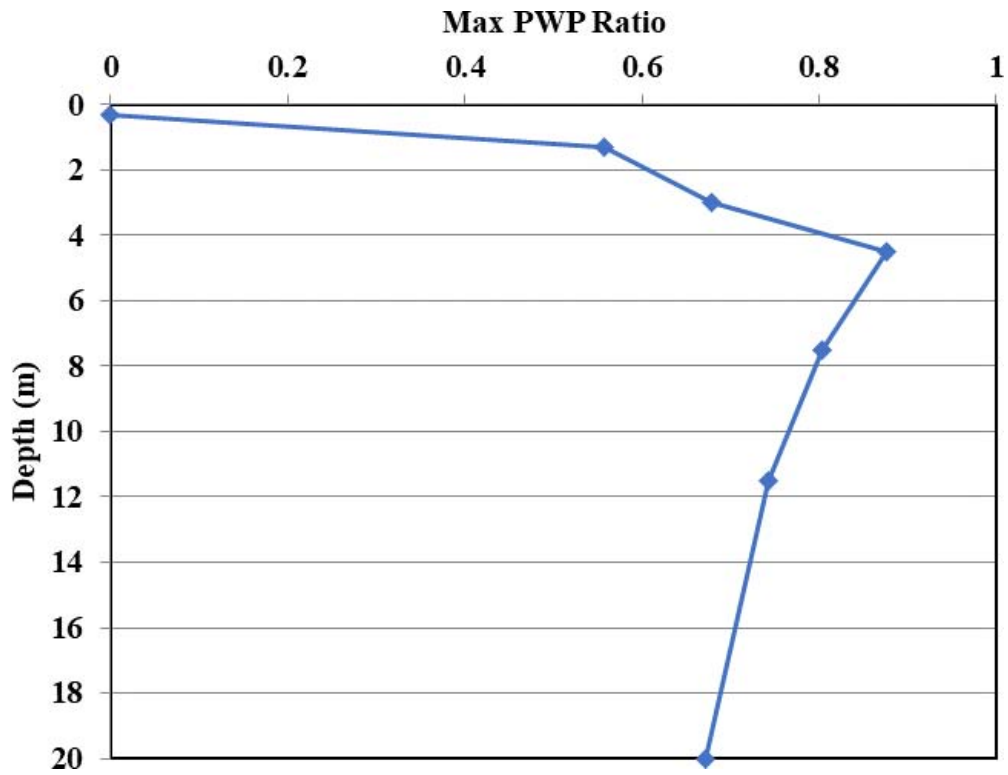


Fig. (13).  $r_u$  value at borehole BH 3.

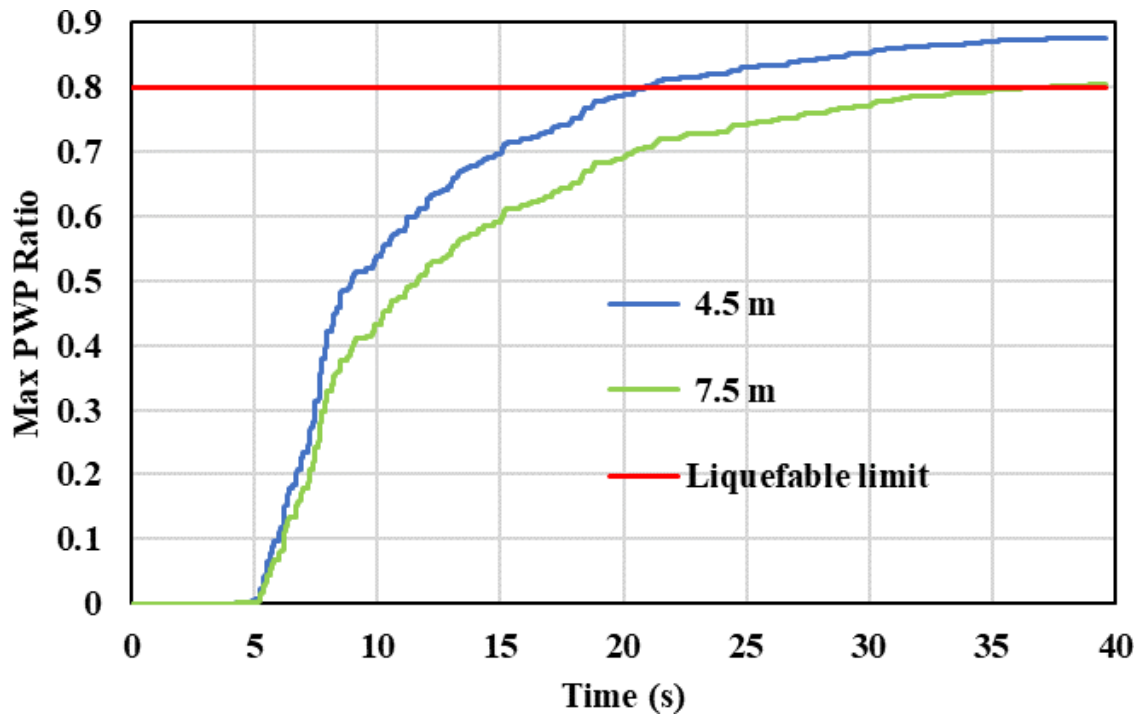


Fig. (14). Time history of  $r_u$  at borehole BH 3.

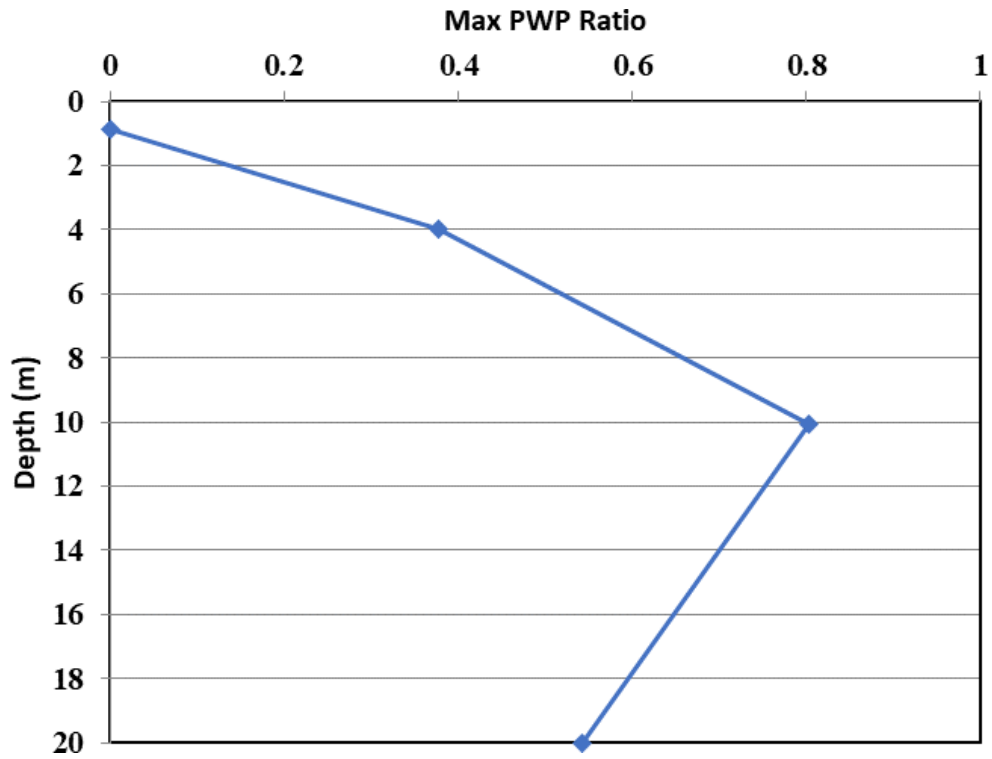


Fig. (15).  $r_u$  value at borehole BH 4.

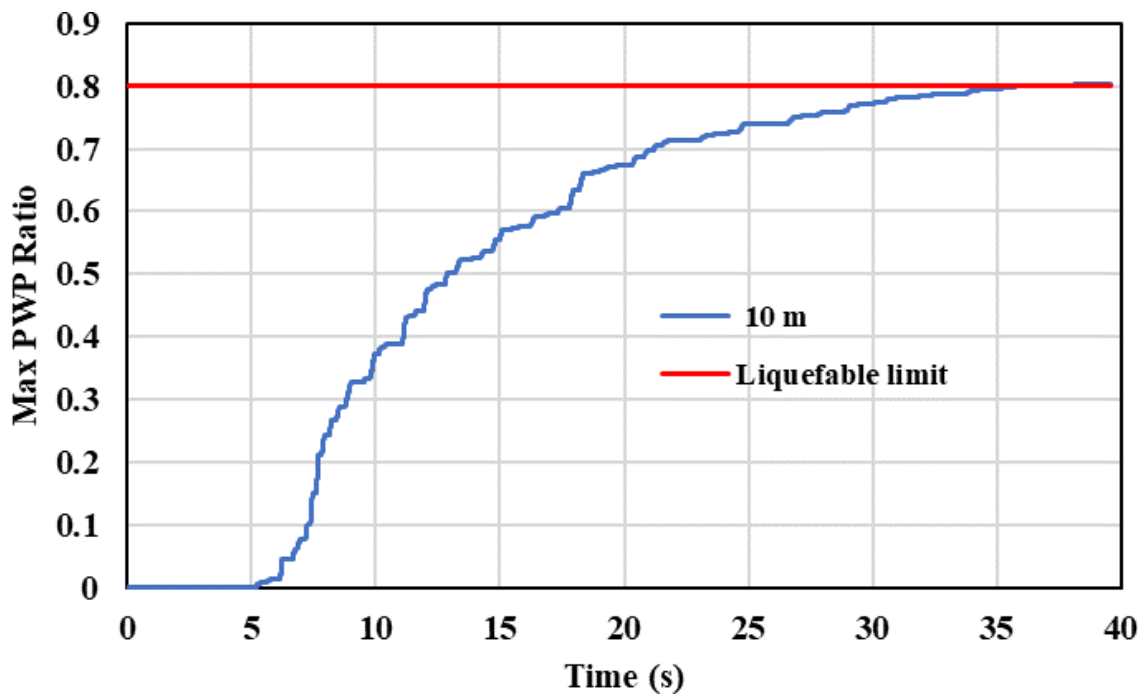


Fig. (16). Time history of  $r_u$  at borehole BH 4.

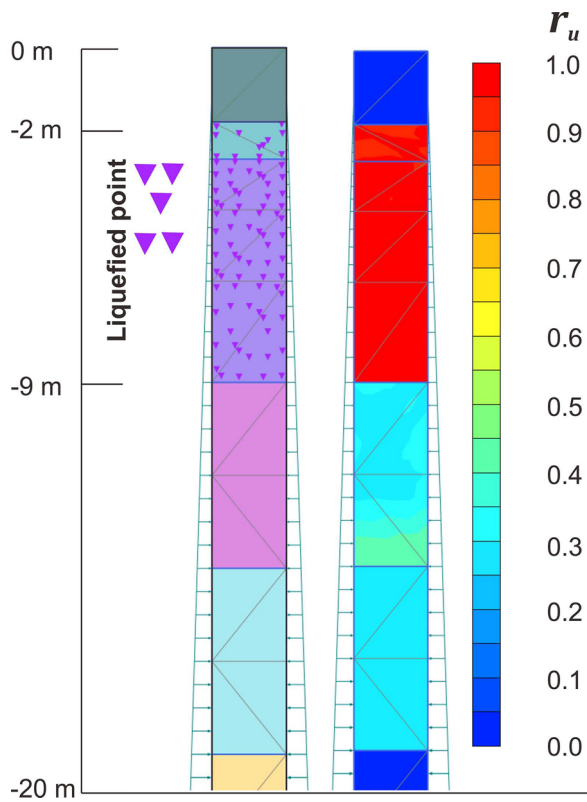


Fig. (17). Liquefied point at borehole BH 1.

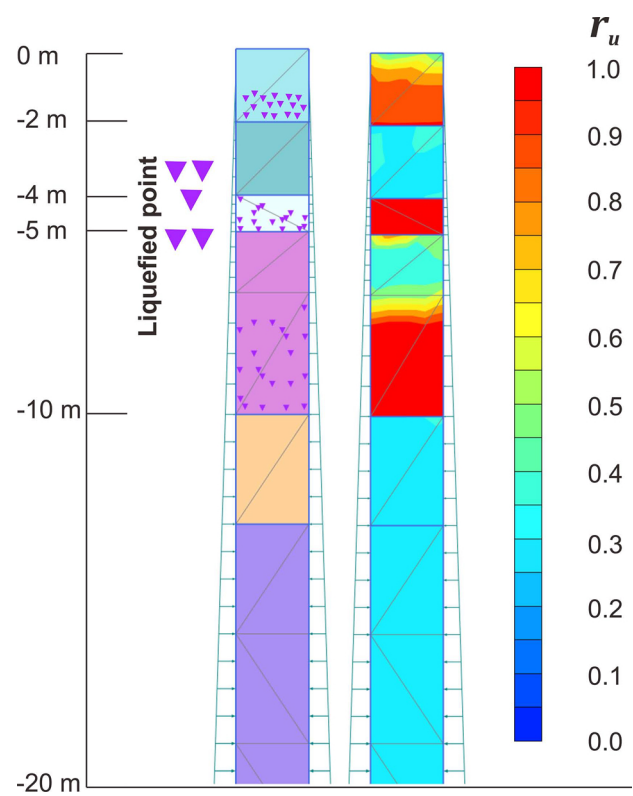


Fig. (19). Liquefied point at borehole BH 3.

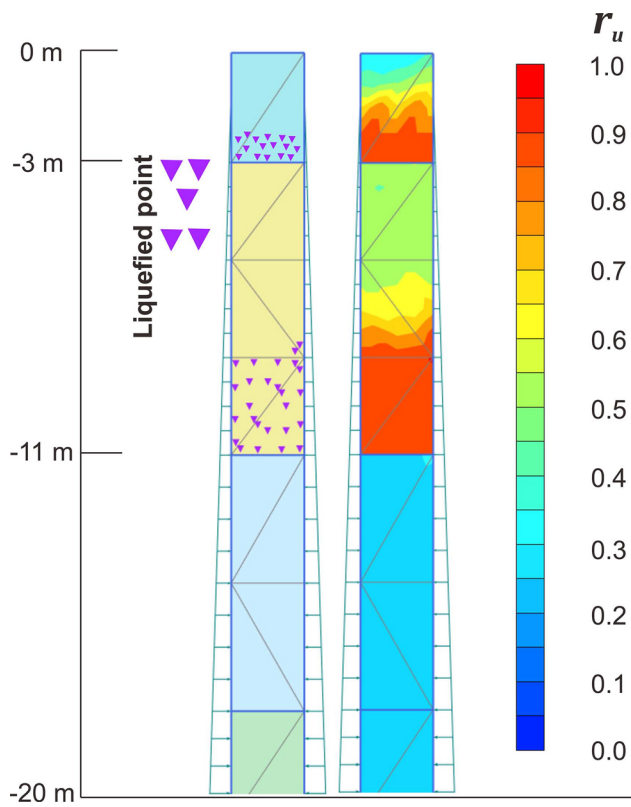


Fig. (18). Liquefied point at borehole BH 2.

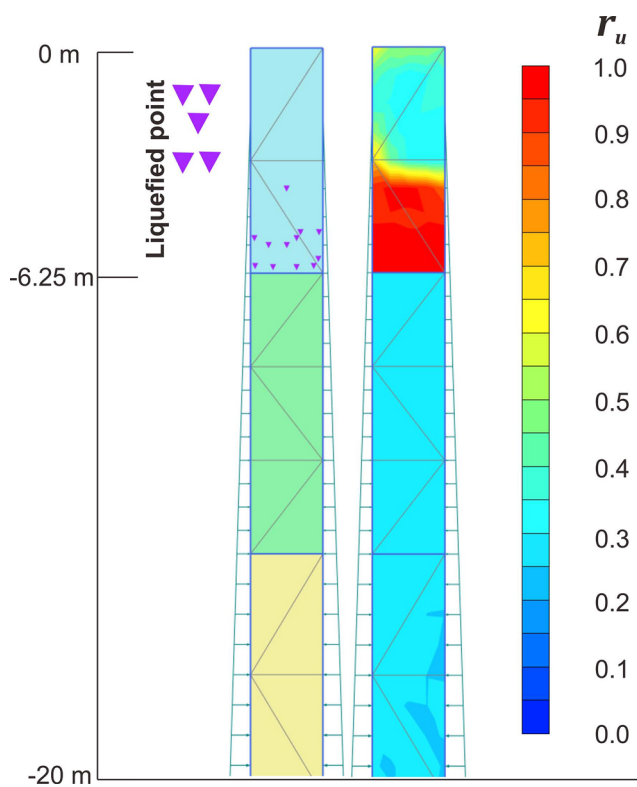


Fig. (20). Liquefied point at borehole BH 4.

## CONCLUSION

The study area is located near the Palu Koro fault line, which is actively moving and results in relatively high earthquake intensity. The shallow groundwater table combined with the unconsolidated sandy lithology in the area makes the study location highly susceptible to the risk of liquefaction.

This study used the earthquake parameters of the Palu earthquake on September 28, 2018, with a magnitude of 7.5 Mw and a PGA value of 0.794g, according to the 2017 earthquake hazard map. For the ground motion input in numerical calculations, the Imperial Valley-06 ground motion was used, sourced from the database at <https://ngawest2.berkeley.edu/>. This ground motion was then matched to align with the site conditions.

The liquefaction analysis was conducted at 4 borehole points using the simplified procedure: BH 1, BH 2, BH 3, and BH 4. At all four boreholes, liquefaction potential was identified at varying depths: for BH 1 at a depth of 17 m, for BH 2 down to 12 m, for BH 3 down to 15 m, and for BH 4 down to 13.5 m. After determining the safety factor against liquefaction potential at each borehole, the pore water pressure increase was calculated using the empirical method by Yegian and Vittelli (1981). In this method, excess pore water pressure values greater than 0.8 indicate the onset of liquefaction. The calculation results demonstrated that the layers with increased pore water pressure exceeding 0.8 matched those experiencing liquefaction, as the calculation parameters were based on the liquefaction safety factor.

The calculation of excess pore water pressure was also conducted using numerical methods with the help of DEEPSOIL v7 and Plaxis 2D software. According to the results from DEEPSOIL v7, for BH 1, layers with a pore pressure ratio ( $r_u > 0.8$ ) were found at depths of 8.5 m and 6.5 m; for BH 2, at depths of 3-11 m; for BH 3, at depths of 4-10 m; and for BH 4, at depths of 6.25-13.95 m, as shown in Table 3.

Calculations using Plaxis 2D were performed for comparison. The results showed that for BH 1, layers with a pore pressure ratio ( $r_u > 0.8$ ) were found at a maximum depth of 9 m; for BH 2, at a maximum depth of 11 m; for BH 3, the deepest layer with  $r_u > 0.8$  was at 10 m, and for BH 4, liquefaction occurred down to a depth of 6.25 m, as detailed in Table 3.

Several interesting findings in this study show that the analysis using the nonlinear method with the DEEPSOIL v7 application produces a single result for each layer. If that layer is liquefied, the entire layer is considered liquefied, regardless of its thickness. In contrast, the analysis using the finite element method with the Plaxis 2D application can yield different values for a single layer. This indicates that the finite element method performs a more detailed analysis and limits the  $r_u$  values according to its critical threshold.

There are significant differences in the calculation of excess pore water pressure. The results of  $r_u$  calculations

using the empirical method indicate that layers experiencing an increase in pore water pressure greater than 0.8 are deeper than the results produced by the non-linear and finite element methods. This discrepancy is related to the use of PGA values: the empirical method uses the peak PGA value for analyzing each layer independently, while the non-linear and finite element calculations adjust the PGA value according to soil conditions and account for the interactions between layers.

The results of this study can be applied to construction projects in areas with similar lithological conditions and groundwater table depths as the study area. Given the potential for soil liquefaction, mitigation measures are essential for any nearby development. It is crucial to anticipate axial bearing capacity issues due to possible negative skin friction and lateral bearing capacity concerns due to potential deformation beyond acceptable limits. These considerations are necessary to ensure the infrastructure built is resilient to liquefaction risks.

## AUTHORS' CONTRIBUTION

It is hereby acknowledged that all authors have accepted responsibility for the manuscript's content and consented to its submission. They have meticulously reviewed all results and unanimously approved the final version of the manuscript.

## LIST OF ABBREVIATIONS

CDSS	=	Cyclic Direct Simple Shear
CRR	=	Cyclic Resistance Ratio
CSR	=	Cyclic Stress Ratio
SPT	=	Standard Penetration Test
PEER	=	Pacific Earthquake Engineering Research Center
MSF	=	Magnitude Scaling Factor
PGA	=	Peak Ground Acceleration

## CONSENT FOR PUBLICATION

Not applicable.

## AVAILABILITY OF DATA AND MATERIALS

The data and supportive information are available within the article.

## FUNDING

This work was financially supported by Ministry of Public Works and Housing of Indonesia, Indonesia (Grant number 21310/UN1/FTK/DTSL/ HK.08.00/2023).

## CONFLICT OF INTEREST

The authors declare no conflict of interest, financial or otherwise.

## ACKNOWLEDGEMENTS

We extend our gratitude to the National Road Implementation Agency (BPJN) of Central Sulawesi

Province, particularly to the Working Unit of National Road Implementation (PJI) Region I, for their support in providing data for this research.

## REFERENCES

- [1] I. Robertson, "StEER: Structural extreme event reconnaissance network palu earthquake and tsunami, Sulawesi, Indonesia field assessment team 1 (FAT-1) early access reconnaissance report (EARR)", Available from: [https://www.researchgate.net/publication/330440517\\_StEER\\_Structural\\_Extreme\\_Event\\_Reconnaissance\\_Network\\_PALU\\_EARTHQUAKE\\_AND\\_TSUNAMI\\_SULAWESI\\_INDONESIA\\_FIELD\\_ASSESSMENT\\_TEAM\\_1\\_FAT-1\\_EARLY\\_ACCESS\\_RECONNAISSANCE\\_REPORT\\_EARR](https://www.researchgate.net/publication/330440517_StEER_Structural_Extreme_Event_Reconnaissance_Network_PALU_EARTHQUAKE_AND_TSUNAMI_SULAWESI_INDONESIA_FIELD_ASSESSMENT_TEAM_1_FAT-1_EARLY_ACCESS_RECONNAISSANCE_REPORT_EARR) [<http://dx.doi.org/10.17603/DS2JD7T>]
- [2] *Map of Indonesia's Liquefaction Vulnerability Zone.*, Ministry of Energy and Mineral Resources, 2019.
- [3] R. Sukanto, H. Sumadra, T. Suptandar, S. Hardjoprawiro, and D. Sudana, *Reconnaissance Geological Map of The Palu Quadrangle, Sulawesi.*, Geological Research and Development Centre: Indonesia, 1973.
- [4] S. Sassa, and T. Takagawa, "Liquefied gravity flow-induced tsunami: First evidence and comparison from the 2018 Indonesia Sulawesi earthquake and tsunami disasters", *Landslides*, vol. 16, no. 1, pp. 195-200, 2019. [<http://dx.doi.org/10.1007/s10346-018-1114-x>]
- [5] M. Munirwansyah, R.P. Munirwan, V. Listia, I. Irhami, and R.P. Jaya, "Sumatra-fault earthquake source variation for analysis of liquefaction in Aceh, Northern Indonesia", *Open Civ. Eng. J.*, vol. 17, no. 1, p. e18741495270939, 2023. [<http://dx.doi.org/10.2174/0118741495270939230921154841>]
- [6] A. Jalil, T.F. Fathani, I. Satyarno, and W. Wilopo, "Nonlinear site response analysis approach to investigate the effect of pore water pressure on liquefaction in Palu", *IOP Conf. Ser. Earth Environ. Sci.*, vol. 871, no. 1, p. 012053, 2021. [<http://dx.doi.org/10.1088/1755-1315/871/1/012053>]
- [7] *Earthquake source and hazard map of Indonesia 2017, Cetakan Pertama. Bandung: National Earthquake Study Center (Indonesia).*, Research and Development Center for Housing and Settlements: Indonesia, 2017.
- [8] D.A. Dayen Siadari, W. Wilopo, and T.F. Fathani, "Seismic microzonation studies in Jogja-Bawen toll road, Magelang Regency, Indonesia", *International Journal of GEOMATE*, vol. 25, no. 110, 2023. [<http://dx.doi.org/10.21660/2023.110.4020>]
- [9] A. Socquet, "Microblock rotations and fault coupling in SE Asia triple junction (Sulawesi, Indonesia) from GPS and earthquake slip vector data", *J. Geophys. Res. Atmos.*, vol. 111, no. B8, p. 2005JB003963, 2006. [<http://dx.doi.org/10.1029/2005JB003963>]
- [10] "National Earthquake Study Center Ministry of Public Works and Public Housing, "Indonesia Earthquake Hazard Deaggregation Map for Earthquake Resistant Infrastructure Planning and Evaluation", Available from: <https://en.antaranews.com/news/262869/ministry-unveils-indonesia-earthquake-hazard-deaggregation-map-book>
- [11] "National Standardization Agency (SNI 2833:2016) Bridge planning for earthquake loads",
- [12] T.L. Youd, "Liquefaction resistance of soils: Summary report from the 1996 Nceer And 1998 Nceer/Nsf", *J. Geotech. Geoenviron. Eng.*, vol. 127, no. 10, pp. 817-833, 2001.
- [13] R. W. Boulanger, and I. M. Idriss, "CPT and SPT based liquefaction triggering procedures", Available from: [https://www.ce.memphis.edu/7137/PDFs/Notes/i3Boulanger\\_Idriss\\_CPT\\_and\\_SPT\\_Liq\\_triggering\\_CGM-14-01\\_20141.pdf](https://www.ce.memphis.edu/7137/PDFs/Notes/i3Boulanger_Idriss_CPT_and_SPT_Liq_triggering_CGM-14-01_20141.pdf)
- [14] M. K. Yegian, and B. M. Vitelli, "Analysis for Liquefaction: Empirical Approach", Available from: <https://bpb-us-e1.wpmucdn.com/sites.northeastern.edu/dist/f/1980/files/2022/10/Analysis-for-Liquefaction-Empirical-Approach.pdf>
- [15] I. Aini, W. Wilopo, and T. Faisal Fathani, "The Correlation of Liquefaction with Excess Pore Water Pressure in Langkat, North Sumatra", *International Journal of GEOMATE*, vol. 26, no. 114, 2024. [<http://dx.doi.org/10.21660/2024.114.4150>]
- [16] L.Z. Mase, "The use of ground motion parameters to identify the liquefaction during a strong earthquake in Northern Thailand", *Civ. Eng. Commun. Media.*, vol. 27, no. 1, pp. 1-8, 2021. [<http://dx.doi.org/10.14710/mkts.v27i1.29218>]
- [17] A. Zakariya, A. Rifa'i, and S. Ismanti, "The correlation of liquefaction potential and probability on excess pore water pressure in kretek 2 bridge area", *J. Civ. Eng. Forum*, vol. 10, no. 1, pp. 39-48, 2023. [<http://dx.doi.org/10.22146/jcef.7002>]
- [18] B. Carlton, "An improved description of the seismic response of sites with high plasticity soils, organic clays, and deep soft soil deposits", University of California, 2014.
- [19] G. Vilhar, R. B. J. Brinkgreve, and L. Zampich, "PLAXIS The PM4Sand model 2018", Available from: <https://research.tudelft.nl/en/publications/plaxis-the-pm4sand-model-2018>
- [20] W. Prakoso, D. Mazaya, and R. A. Kartika, "Pore pressure responses of liquefied numerical sand columns", *J. Civ. Eng. Forum.*, vol. 8, no. 3, pp. 225-236, 2022. [<http://dx.doi.org/10.22146/jcef.3395>]
- [21] I. M. Idriss, and R. W. Boulanger, "Soil Liquefaction During Earthquakes", Available from: <https://istasazeh-co.com/wp-content/uploads/2023/02/Soil-Liquefaction-During-Earthquakes-M.-Idriss-and-Ross-W.-Boulanger.pdf>
- [22] R. W. Boulanger, and K. Ziotopoulou, "Pm4sand (Version 3): A sand plasticity model for earthquake engineering applications", Available from: [https://faculty.engineering.ucdavis.edu/boulanger/wp-content/uploads/sites/71/2014/09/Boulanger\\_Ziotopoulou\\_PM4Sand\\_Model\\_CG-M-15-01\\_2015.pdf](https://faculty.engineering.ucdavis.edu/boulanger/wp-content/uploads/sites/71/2014/09/Boulanger_Ziotopoulou_PM4Sand_Model_CG-M-15-01_2015.pdf)
- [23] R.W. Day, *Geotechnical Earthquake Engineering Engineering Handbook.*, 2nd ed McGraw-Hill Professional: New York, 2012.
- [24] T. Iwasaki, K. Tokida, and F. Tatsuoka, "Soil liquefaction potential evaluation with use of the simplified procedure", *International Conferences on Recent Advances in Geotechnical Earthquake Engineering and Soil Dynamics* St. Louis, Missouri, 1981